Available online at www.sciencedirect.com
SCIENCE DIRECT®
Journal of Solid State Chemistry 178 (2005) 2980–2986
JOURNAL OF SOLID STATE CHEMISTRY
www.elsevier.com/locate/jssc

A surface modification scheme for incorporation of nanocrystals in mesoporous silica matrix

Lan Zhao, Guangshan Zhu, Daliang Zhang, Yue Chen, Shilun Qiu*

State Key Laboratory of Inorganic Synthesis and Preparative Chemistry, College of Chemistry, Jilin University, Changchun 130012, People's Republic of China

Received 13 May 2005; received in revised form 24 June 2005; accepted 28 June 2005
Available online 15 August 2005

Abstracts

A simple surface modification scheme is proposed to introduce various nanocrystals including oil-soluble Au nanocrystals, water-soluble Au nanocrystals and magnetic γ-Fe_2O_3 nanocrystals into mesoporous silica matrix. Disordered mesostructured cellular foam (MCF) and well-ordered FDU-12 were used as matrix materials. Surface modification of mesoporous silica with particular ligands enhanced the interaction between the matrix and nanocrystals, thereby facilitating the incorporation. High loading (up to 20% in weight) and uniform distribution of nanocrystals in mesopores were observed by transmission electron microscopy (TEM). The physical and chemical properties of nanocrystals were well maintained during this process. Moreover, the obtained composites were still highly porous with pore volume more than 1.0 cm^3/g, as evidenced by N_2 adsorption experiments.

Keywords: Mesoporous materials; Nanoparticles

1. Introduction

The synthesis and applications of various nanocrystals have emerged as one of the most important fields in material science. Their unique optical, electrical, magnetic and catalytic properties cannot be achieved by bulk materials. The properties of these nanocrystals are closely related to their particle size, shape, crystallinity and aggregation degree. For example, the optical properties of gold nanocrystals can be finely adjusted by changing their particle size or particle shape [1]; iron oxide nanocrystals may lose their specific properties associated with single domain magnetic nanostructures if they aggregate into large clusters. To keep nanocrystals well dispersed without aggregation and to improve their chemical stability, as required in most applications, people usually use inert materials such as silica to fabricate a coating on the surface of nanocrystals [2–5]. Mesoporous silica materials can naturally act as host matrix for various nanocrystals, since they provide robust, inert and open frameworks with tunable pore size in nanometer scale. A successful incorporation of nanocrystals in mesoporous silica matrix can well maintain the physical and chemical properties of nanocrystals and improve their stability at the same time, as achieved by silica coating [6–14]. Moreover, the obtained nanocrystals/mesoporous silica composites are still porous with large surface area and well-defined nanopores, which can be used as multi-functional materials.

The dominant strategy for synthesizing such composites has been to in situ grow the nanocrystals inside the pores of the mesoporous silica. For example, noble metals including Au, Ag and Pt nanowires have been prepared through a wetness impregnation route followed by thermal decomposition in the channels of SBA-15 [7,8]; Au nanocrystals were prepared in the cages of FUD-12 according to a similar impregnation method [15]; PbS nanocrystals and nanowires were

*Corresponding author. Fax: +86 431 5168659.
E-mail address: sqiu@mail.jlu.edu.cn (S. Qiu).

0022-4596/$ - see front matter © 2005 Elsevier Inc. All rights reserved.
doi:10.1016/j.jssc.2005.06.040

fabricated by combining the functionalizations of SBA-15 surface with thiol groups, absorption of Pb^{2+} and heating in a N_2 atmosphere [16]. As summarized in a recent review, many other approaches have also been exploited to prepare various nanocrystal/mesoporous silica composites [17].

In these examples, however, the loading amount of nanocrystals has been limited. It can be possibly explained by that the grown nanocrystals inside the porous system would restrict further transport of feedstock materials. This same reason resulted in the difficulty to produce nanocrystals uniform both in size and in morphology. Since the properties of nanocrystals are always size-dependent and morphology-dependent, new methods for preparing nanocrystal/mesoporous silica composites are needed to achieve high loading and high quality of nanocrystals.

On the other hand, there are many well-developed synthetic methods, through which various nanocrystals with narrow size and shape distributions can be prepared. An alternative strategy for the creation of nanocrystal/mesoporous silica composites is to synthesize nanocrystals and mesoporous silica separately and then incorporate preformed nanocrystals into the mesoporous matrix. In this way, the nanocrystals are synthesized externally, so their morphology could be controlled more accurately. Several examples have been reported that nanocrystals can be used as template for mesoporous silica synthesis to obtain nanocrystal/mesoporous silica composites [6,18,19]. However, due to the lack of affinity between them, it is difficult to directly introduce the pre-synthesized nanocrystals into the mesoporous silica materials densely and uniformly. In most cases, the nanocrystals are just adhered on the surface of mesoporous silica particles rather than entrapped inside the mesopores.

To prevent nanocrystals from aggregation, passivating ligands such as aliphatic amines [20], thiols [21] and fatty acids [22], which cover the surface of nanocrystals, are generally used for the synthesis of nanocrystals. Also, nanocrystals could be made to be either oil-soluble or water-soluble, depending on the terminal groups of the ligands used [20]. Herein we describe a simple surface modification scheme that enables the incorporation of nanocrystals in the mesoporous silica matrix. The whole procedure consists of two steps: First, the surface of mesoporous silica is modified by particular functional groups that have suitable interactions (hydrophobic interaction or covalent bond) with the ligands on nanocrystals. Second, the modified mesoporous silica is mixed with nanocrystal solution, followed by evaporating the solvents under vacuum. Through this approach, we have successfully incorporated magnetic γ-Fe_2O_3 nanocrystals and Au nanocrystals in mesostructured cellular foam (MCF) [23], as well as Au nanocrystals in highly ordered FUD-12 [15].

2. Experimental

2.1. Incorporation of Au nanocrystals in MCF

MCF was synthesized according to literature [23] and the organic template was removed by calcination. The hydrophobic modification of MCF with long alkyl (octyl) chains was carried out as follows: After degassing at 150 °C under vacuum overnight, 1.0 g of calcined MCF was suspended in 20 mL of toluene. Then 0.6 mL of triethylamine (4.0 mmol) and 0.45 mL of chlorodimethyloctylsilane (2.0 mmol) were added sequentially with stirring. The suspension was stirred at 60 °C for 24 h and then filtered. The solid was washed with portions of toluene for several times and dried under vacuum. The modified MCF is termed MCF-C_8. Oil-soluble Au nanocrystals coated with dodecanethiol ligands were synthesized according to literature [20]. A total of 20 mg of Au nanocrystals were dispersed in 10 mL of toluene by sonication, followed by the addition of 0.1 g of MCF-C_8. The resulting mixture was stirred at room temperature overnight. The solvent was then removed under vacuum (70 mbar) at 40 °C using a rotary evaporator. The resulting solid was suspended in 5 mL of toluene by stirring and was evaporated again. This operation was repeated for several times. Finally, the solid was fully washed by toluene to get Au nanocrystals/MCF composite.

2.2. Incorporation of magnetic γ-Fe_2O_3 nanocrystals in MCF

Magnetic γ-Fe_2O_3 nanocrystals coated with oleic-acid ligands were synthesized according to literature that could be well dispersed in hydrocarbon solvents [22]. MCF-C_8 was employed as matrix material. 40 mg of γ-Fe_2O_3 nanocrystals was dispersed in 10 mL of toluene by sonication, followed by addition of 0.1 g of MCF-C_8. The resulting mixture was stirred at room temperature overnight. The solvent was then removed under vacuum (70 mbar) at 40 °C using a rotary evaporator. The solid was suspended in 5 mL of toluene by stirring and evaporated again. This operation was repeated for several times. Finally, the solid was fully washed by toluene to get γ-Fe_2O_3 nanocrystals/MCF composite.

2.3. Incorporation of Au nanocrystals in FUD-12

Water-soluble Au nanocrystals coated with mercaptopropanic acid ligands were synthesized according to literature [20]. Highly ordered mesoporous silica FUD-12 was synthesized according to literature [15]. In order to facilitate the incorporation of Au nanocrystals, the entrance size of FDU-12 was enlarged via a relatively high aging temperature (120 °C) [15]. FDU-12 was further modified with amine groups by reacting with 3-

aminopropyltriethoxysilane (APS). Typically, 1.0 g of calcined FDU-12 was suspended in 20 mL of toluene, followed by addition of 2.0 mmol of APS with stirring. The suspension was stirred at 60 °C for 24 h and then filtered. The resulting solid was washed with toluene for several times and dried under vacuum. The modified FDU-12 is termed FUD-12-NH_2. A total of 0.1 g FUD-12-NH_2 was added to a 10 mL aqueous solution containing 20 mg of Au nanocrystals. The resulting mixture was stirred at room temperature overnight. Water was slowly removed under vacuum (70 mbar) at 40 °C through a rotary evaporator to get Au nanocrystals/FDU-12 composite.

2.4. Characterization

The nitrogen adsorption/desorption isotherms were measured using a Micromeritics ASAP 2020 M system. The samples were degassed for 10 h at 200 °C before the measurements. Fourier transform infrared spectroscopy (FT-IR) measurements were conducted using FTS 7000 series. UV–visible (vis) spectrum of the Au nanocrystals in toluene solution was measured with a Hitachi U-3310 UV–vis spectrophotometer. The diffuse reflectance UV–vis spectrum of the Au/MCF composite was measured with spectrometer of PE Lambda 20, and $BaSO_4$ was an internal standard sample. Transmission electron microscopy (TEM) experiments were performed on a JSM-3010 electron microscope (JEOL, Japan) with an acceleration voltage of 300 kV.

3. Results and Discussion

MCF is a novel mesoporous silica material templated by oil-in-water microemulsions [23]. The ultra-large mesopores have made MCF particularly useful as catalyst supports and separation media for processes involving large substrate. Previous studies illustrate that MCF has uniform, cage-like mesopores with entrances (or "windows") narrower than the diameter of the cage itself. The calcined MCF in this work showed a type IV N_2 adsorption–desorption isotherm (Fig. 1a) from which its pore diameter and window diameter were determined to be 28.5 and 14.8 nm, respectively, according to the BdB–FHH method [24]. The BET surface area was 535 m^2/g and the pore volume was 2.1 cm^3/g. The modification of MCF with hydrophobic alkyl (C_8) groups decreased both pore diameter and window diameter by ~2 nm, so did the surface area (345 m^2/g) and pore volume (1.6 cm^3/g). However, the isotherm did not change in shape after modification and the pore size distribution was still very narrow (Fig. 1b), suggesting a uniform coverage of C_8 groups on MCF surface. The success of surface modification with long-chain alkyl groups was also evidenced by FT-IR

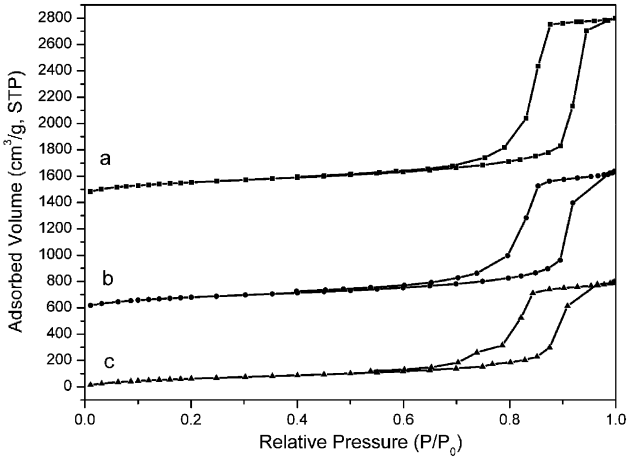

Fig. 1. N_2 adsorption/desorption isotherms of (a) MCF, (b) MCF-C_8, and (c) Au/MCF-C_8 composite. For clarify, the isotherms of MCF-C_8 and Au/MCF-C_8 composite are offset by 600 and 1400 along the *y*-axis, respectively.

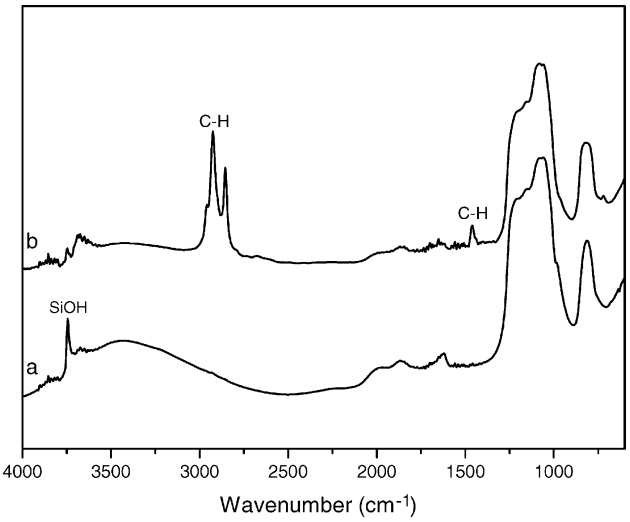

Fig. 2. FTIR spectra of (a) MCF and (b) MCF-C_8.

spectroscopy. Calcined MCF showed a typical FTIR spectrum of bare silica (Fig. 2a). After modification with C_8 groups, it exhibited new peaks around 2900 and 1450 cm^{-1} that are associated with C–H vibration, while the peak of silanol (SiOH) groups at 3750 cm^{-1} disappeared (Fig. 2b). The weight percent of C_8 groups in modified MCF was 10% (1.3 mmol ligand/g of silica), as calculated by element analysis.

Peng and co-worker have reported a single-phase route toward the synthesis of monodispersed Au nanocrystals [20]. Due to the weak ligands used in that synthetic scheme, the surface modification of the as-synthesized Au nanocrystals was quite straightforward through ligand exchange. Depending on the terminal groups of the ligands, Au nanocrystals can be either oil-soluble or water-soluble. For example, oil-soluble Au

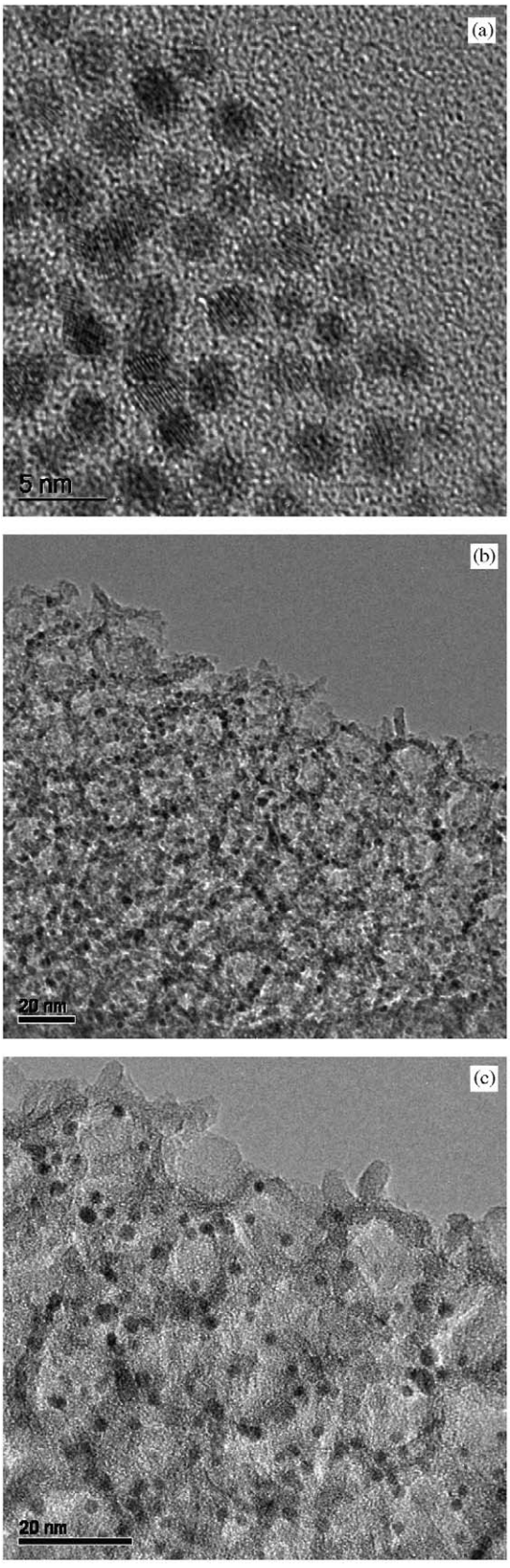

Fig. 3. (a) High-resolution TEM micrograph of the pre-synthesized Au nanocrystals; (b) TEM micrograph of the Au/MCF-C_8 composite at low magnification; (c) TEM micrograph of the Au/MCF-C_8 composite at high magnification.

nanocrystals can be prepared by surface modification with dodecanethiol ligands, while mercaptopropanic acid ligands can make them soluble in water.

In this study, we prepared hydrophobic Au nanocrystals dispersed in toluene according to Peng's method [20]. These Au nanocrystals are uniform in size (4 nm) and highly crystalline as illustrated by the high-resolution TEM image (Fig. 3a). Being extremely hydrophobic, MCF-C_8 was readily immersed in the toluene solution of Au nanocrystals. A solvent evaporation process was employed to promote Au nanocrystals to enter the mesopores of MCF-C_8, followed by washing with toluene to remove the residual nanocrystals on the surface. Element analysis of the product gave 15% of Au content in weight. Although due to the presence of non-porous nanocrystals this Au nanocrystals/MCF composite showed lower surface area and pore volume than parent material MCF-C_8, it was still highly porous with 270 m^2/g surface area and 1.2 cm^3/g pore volume. The N_2 adsorption isotherm of the composite was not smooth in the desorption branch and the BJH pore size distribution was relatively broad (Fig. 1c). These results suggested that Au nanocrystals were entrapped in the mesopores that would partially block the pore system. TEM image (Fig. 3b) showed that the dispersion of Au nanocrystals was dense and uniform. High-resolution TEM image further revealed that Au nanocrystals were incorporated in the foam-like mesopores of MCF rather than on the surface of MCF particle (Fig. 3c).

The UV–vis spectrum of the toluene solution of Au nanocrystals employed in this work was shown in Fig. 4a. A plasmon resonance band at 520 nm exhibited the character of nano-sized Au crystals [6,25]. Correspondingly, the diffuse reflectance UV–vis spectrum of the Au/MCF composite showed an obvious band at the same region (Fig. 4b), suggesting that the optical

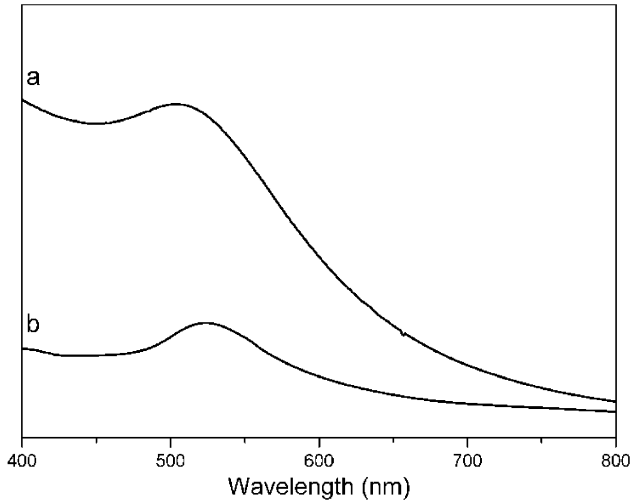

Fig. 4. (a) UV–vis spectrum of the toluene solution of Au nanocrystals; (b) diffuse reflectance UV–vis spectrum of the Au/MCF-C_8 composite.

property of Au nanocrystals was unaffected during the incorporation process.

Notably, the surface modification of MCF with C_8 groups is essential towards incorporating oil-soluble Au nanocrystals. If unmodified MCF is used as host material, only low loading amount ($< 5\%$ in weight) can be achieved. It is believed that the incorporation is promoted by the hydrophobic interaction between the C_8 groups on silica surface and the alkyl chains of dodecanethiol ligands on Au nanocrystals. In addition, the minus pressure used for solvent evaporation produces capillary force in mesopores that is also helpful for entrapping more nanocrystals. If the incorporation were carried out under normal pressure, the loading amount of nanocrystals would be about 10%, much less than that through solvent evaporation.

Since various noble nanocrystals, such as Ag, Pd and Pt, can be synthesized from the same route [20], they are readily introduced in mesoporous silica via this surface modification scheme. The obtained composites can be used as heterogeneous catalysts for different reactions. Since the nanocrystals introduced in this way are well dispersed in pores, the resulting catalysts will be active and stable.

This surface modification scheme could also be extended to introduce other oil-soluble nanocrystals, e.g. magnetic γ-Fe_2O_3 nanocrystals, into hydrophobic mesoporous matrix. Magnetic γ-Fe_2O_3 nanocrystals were synthesized by thermal decomposition of iron pentacarbonyl in the presence of oleic acid ligands, followed by controlled oxidation with trimethylamine oxide, as reported by Hyeon et al. [22]. These nanocrystals are very uniform in size ($\sim$7 nm) with hexagonal shape (Fig. 5a). During solvent evaporation, γ-Fe_2O_3 nanocrystals were successfully incorporated in MCF-C_8 matrix with a high loading of 20% in weight, which could also be attributed to the hydrophobic interaction between the C_8 groups on silica surface and the alkyl chains of oleic ligands on γ-Fe_2O_3 nanocrystals. The bright-field and dark-field TEM images of the same area of the γ-Fe_2O_3/MCF-C_8 composite are shown in Fig. 5b and Fig. 5c, respectively. Since the sample is thick, the bright-field image is not very informative. However, the dark-field image clearly indicates that the magnetic γ-Fe_2O_3 nanocrystals were uniformly and densely distributed in MCF matrix. The bright spots in the dark-field image correspond to the γ-Fe_2O_3 nanocrystals (Fig. 5c). The obtained γ-Fe_2O_3 nanocrystals/MCF composite has a BET surface area of 220 m^2/g and total pore volume of 1.0 cm^3/g, as calculated from N_2 adsorption isotherm.

Possessing magnetic property and significant porosity simultaneously, the γ-Fe_2O_3 nanocrystals/MCF composite exhibits great potential in many applications. For example, it will be useful for heterogeneous catalysis as a catalyst support that can be easily separated from the

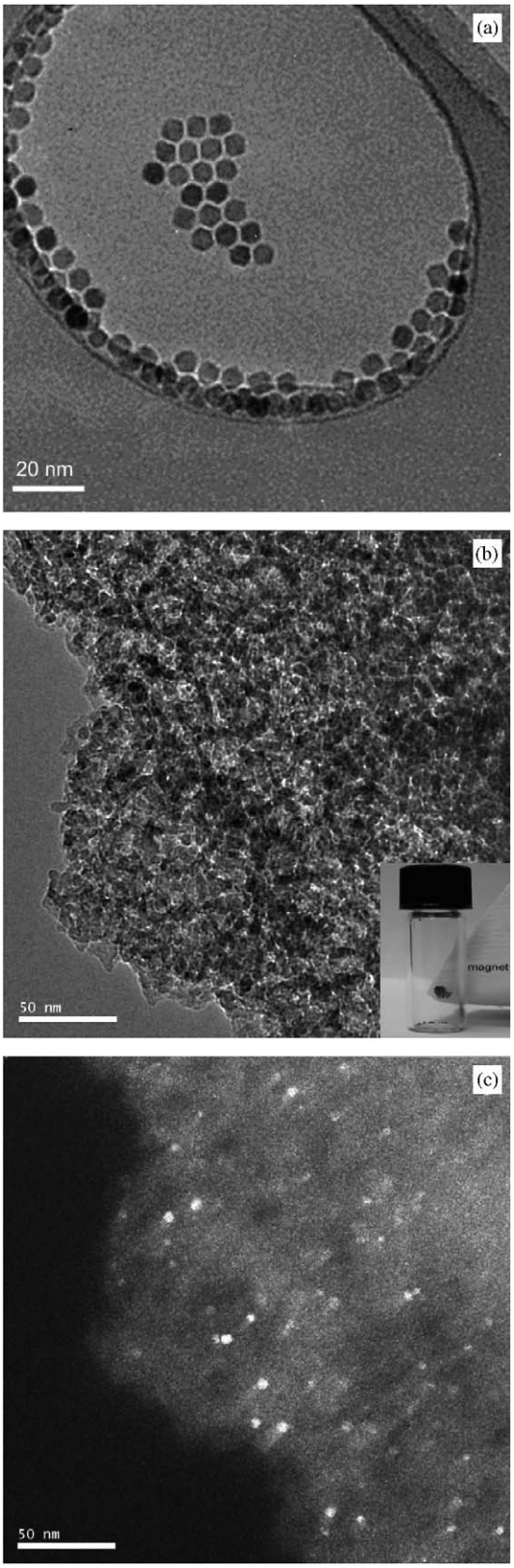

Fig. 5. (a) TEM micrograph of the pre-synthesized magnetic γ-Fe_2O_3 nanocrystals; (b) Bright-field TEM micrograph and (c) Dark-field TEM micrograph of the same area of the γ-Fe_2O_3/MCF-C_8 composite. Inset is a photograph showing the magnetically collectable property of the γ-Fe_2O_3/MCF-C_8 composite.

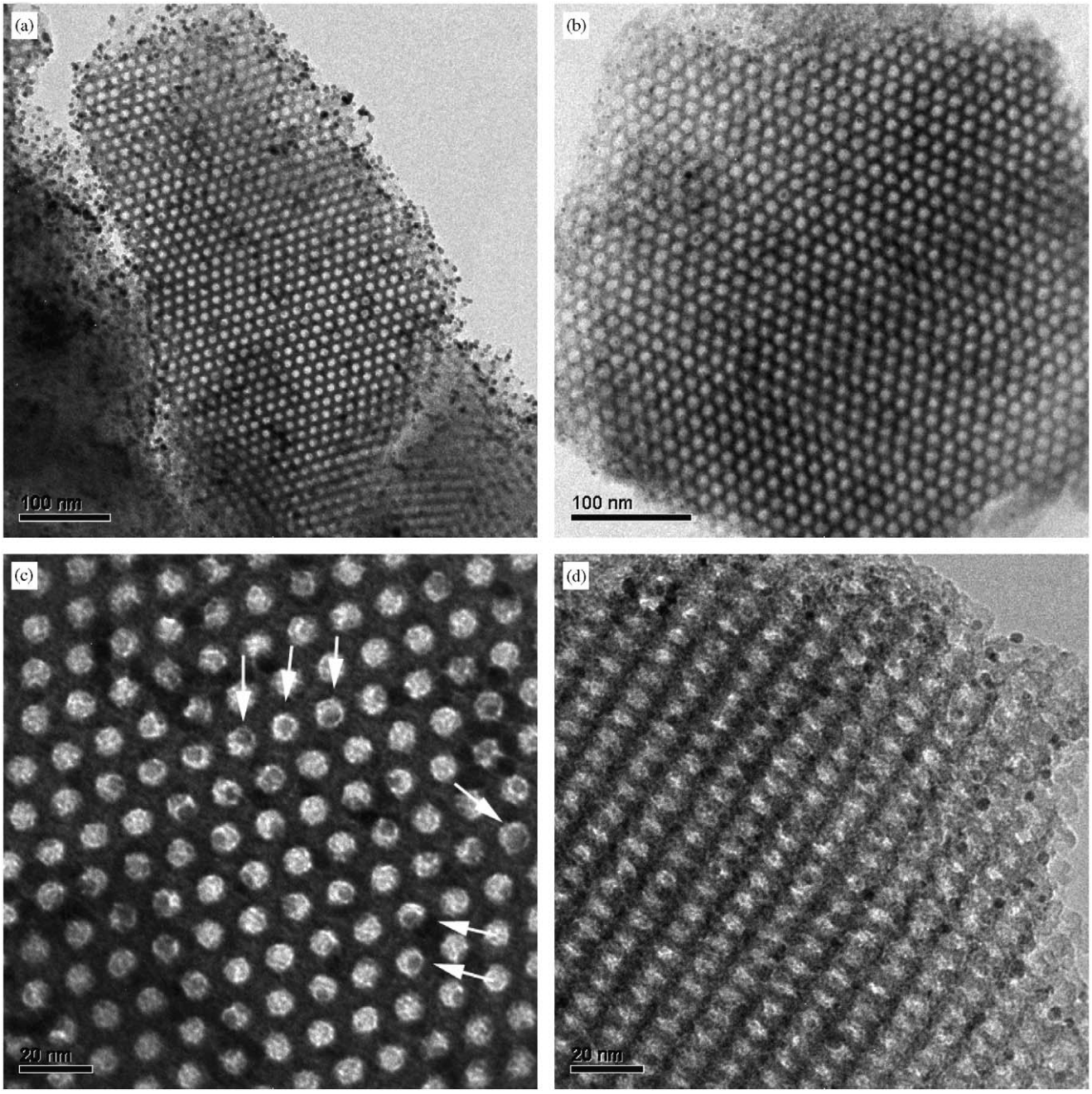

Fig. 6. (a) TEM micrograph of Au nanocrystals in FDU-12 functionalized with amine groups on both inner and outer surface. (b) TEM micrograph of Au nanocrystals in FDU-12 functionalized with amine groups only on inner pore surface. High magnification TEM images of the same sample with (b) taken in different incidence: (c) [110] and (d) [211]. Arrows in (c) indicates some of the Au nanocrystals entrapped in the mesopores.

reaction system by magnetic field. Its magnetic separability was illustrated in Fig. 5 (inset) where a magnet was successfully employed to extract the composite powder out from solution.

The surface modification method is also applicable for incorporating nanocrystals into ordered mesoporous silica, e.g. FDU-12 with a face-centered cubic mesostructure (*Fm*-3*m*). Water-soluble Au nanocrystals (~4 nm) with mercaptopropanic acid protective ligands are incorporated in this case, which were synthesized according to Peng's route [20]. Accordingly, we modified FDU-12 with amine groups (by reacting with 3-APS) to entrap the Au nanocrystals through strong acid–base interaction between carboxyl groups and amine groups. TEM image (Fig. 6a) indicated that in this way a large amount of Au nanocrystals could be attached to FDU-12. However, unlike the cases described above, the Au nanocrystals were located not only in the mesopores but

also on the outer surface of FDU-12 particles, because the presence of amine groups on silica surface would catch Au nanocrystals. The incorporation of Au nanocrystals exclusively in mesopores could be achieved by a three-step procedure. First, trimethylchlorosilane was used to react with as-synthesized FDU-12 (with surfactant template in the pores) to passivate the outer surface by $Si(CH_3)_3$ (TMS) groups. Second, surfactant templates were removed by solvent extraction. Last, template-free FDU-12 was reacted with APS to functionalize the inner surface. In this way, only inner surface of FDU-12 was functionalized with alkyl amine groups, while the outer surface was kept inactive to Au nanocrystals. Similar scheme has been employed by Lin et al. to synthesize Pt nanoclusters in the pore channels of SBA-15 [17]. Using the obtained FDU-12-NH_2 as matrix, Au nanocrystals were mostly incorporated in the mesopores as evidenced by TEM image (Fig. 6b). The high-resolution TEM images of Au-incorporated FDU-12 taken in [110] and [211] incidences are shown in Fig. 6c and d, respectively. From these images the distribution of Au nanocrystals in mesoporous matrix can be observed clearly. As indicated by the arrows in Fig. 6c, Au nanocrystals are indeed in the mesopores and separated from each other by pore walls. In certain local regions, the Au nanocrystals form ordered arrays based on how the mesopores are arranged, which implies the potential use of this Au/FDU-12 composite in novel optical and electronic applications. Also, the TEM images reveal that both the morphology of Au nanocrystals and the highly ordered mesostructure of FDU-12 have been well maintained during the incorporation process.

4. Conclusions

We have proposed a simple surface modification scheme for incorporating different nanocrystals in mesoporous silica matrix to prepare nanocrystals/mesoporous silica composites. This approach is generally effective for various nanocrystals, including oil-soluble Au nanocrystals, water-soluble Au nanocrystals, and magnetic γ-Fe_2O_3 nanocrystals, as well as mesoporous silica materials with different structures. Since the nanocrystals are externally synthesized, their morphologies and properties can be accurately controlled. This method shows little influence on the physical and chemical properties of the incorporated nanocrystals. Also, the structure and porosity of the matrix material have been well maintained. The obtained multi-functional composites show potential applications in catalysis, separation and optical/electronic device.

References

[1] E. Hao, R.C. Bailey, G.C. Schatz, J.T. Hupp, S. Li, Nano Lett. 4 (2004) 327.
[2] Y. Lu, Y. Yin, B.T. Mayers, Y. Xia, Nano Lett. 2 (2002) 183.
[3] Y. Lu, Y. Yin, Z. Li, Y. Xia, Nano Lett. 2 (2002) 785.
[4] L.M. Liz-Marzan, M. Giersig, P. Mulvaney, Langmuir 12 (1996) 4329–4335.
[5] C.R. Vestal, Z.J. Zhang, Nano Lett. 3 (2003) 1739.
[6] H. Fan, K. Yang, D.M. Boye, T. Sigmon, K.J. Malloy, H. Xu, G.P. Lopez, C.J. Brinker, Science 304 (2004) 567.
[7] Y.-J. Han, J.M. Kim, G.D. Stucky, Chem. Mater. 12 (2000) 2068.
[8] M.H. Huang, A. Choudrey, P. Yang, Chem. Commun. 12 (2000) 1063.
[9] H.J. Shin, R. Ryoo, Z. Liu, O. Terasaki, J. Am. Chem. Soc. 123 (2001) 1246.
[10] A. Fukuoka, N. Higashimoto, Y. Sakamoto, S. Inagake, Y. Fukushima, M. Ichikawa, Micropor. Mesopor. Mater. 48 (2001) 171.
[11] W. Zhou, J.M. Thomas, D.S. Shephard, B.G. Johnson, D. Ozkaya, T. Maschmeyer, R.G. Bell, Q. Ge, Science 280 (1998) 705.
[12] A. Fukuoka, Y. Sakamoto, S. Guan, S. Inagaki, N. Sugimoto, Y. Fukushima, K. Hirahara, S. Iilima, M. Ichikawa, J. Am. Chem. Soc. 123 (2001) 3373.
[13] H. Winkle, A. Brikner, V. Hange, I. Wolf, R. Schmechel, H. von Seggern, R.A. Fischer, Adv. Mater. 11 (1999) 1444.
[14] A.F. Gross, M.R. Diehl, K.C. Beverly, E.K. Richman, S.H. Tolbert, J. Phys. Chem. B 107 (2003) 5475.
[15] J. Fan, C. Yu, F. Gao, J. Lei, B. Tian, L. Wang, Q. Luo, B. Tu, W. Zhou, D. Zhao, Angew. Chem. Int. Ed 42 (2003) 3146.
[16] Q. Lu, F. Gao, D. Zhao, Nano Lett. 2 (2002) 823.
[17] J. Shi, Z. Hua, L. Zhang, J. Mater. Chem. 14 (2004) 795.
[18] Z. Konya, V.F. Puntes, I. Kiricsi, J. Zhu, A.P. Alivisatos, G.A. Somorjai, Nano Lett. 2 (2002) 907.
[19] Z. Konya, V.F. Puntes, I. Kiricsi, J. Zhu, J.W. Ager III, M.K. Ko, H. Frei, P. Alivisatos, G.A. Somorjai, Chem. Mater. 15 (2003) 1242.
[20] N.R. Jana, X. Peng, J. Am. Chem. Soc. 125 (2003) 14280.
[21] M. Brust, M. Walker, D. Bethell, D.J. Schiffirn, R. Whyman, J. Chem. Soc. Chem. Commun. (1994) 801.
[22] T. Hyeon, S.S. Lee, J. Park, Y. Chung, H.B. Na, J. Am. Chem. Soc. 123 (2001) 12798.
[23] P. Schmidt-Winkel, P. Yang, D.I. Margolese, J.S. Lettow, J.Y. Ying, G.D. Stucky, Chem. Mater. 12 (2000) 686.
[24] W.W. Jr. Lukens, P. Schmidt-Winkel, D. Zhao, J. Feng, G.D. Stucky, Langmuir 15 (1999) 5403.
[25] T. Shimizu, T. Teranishi, S. Hasegawa, M. Miyake, J. Phys. Chem. B 107 (2003) 2719.